Holocene landscape dynamics in the Ghaggar-Hakra palaeochannel region at the northern edge of the Thar Desert, northwest India

Julie A. Durcan[1]*, David S.G. Thomas[1], Sanjeev Gupta[2], Vikas Pawar[3], Ravindra N. Singh[4], Cameron A. Petrie[5]

[1]School of Geography and the Environment, University of Oxford, Oxford, UK
[2]Department of Earth Science and Engineering, Imperial College London, UK
[3]Department of History, M.D. University, Rohtak, India.
[4]Department of AIHC and Archaeology, Banaras Hindu University, Varanasi, India
[5]Division of Archaeology, University of Cambridge, UK

*Corresponding author: julie.durcan@ouce.ox.ac.uk

Abstract

Precession-forced change in insolation has driven de-intensification of the Asian Monsoon systems during the Holocene. Set against this backdrop of a weakening monsoon, Indus Civilisation populations occupied a number of urban settlements on the Ghaggar-Hakra plains during the mid-Holocene from 4.5 ka until they were abandoned by around 3.9 ka. Regional climatic variability has long been cited as a potential factor in the transformation of Indus society, however there remain substantial gaps in the chronological framework for regional climatic and environmental change at the northern margin of the Thar Desert. This makes establishing a link between climate, environment and society challenging. This paper presents 24 optically stimulated luminescence ages from a mixture of 11 fluvial and aeolian sedimentological sites on the Ghaggar-Hakra floodplain/interfluve, an area which was apparently densely populated during the Indus urban phase and subsequently. These ages identify fluvial deposition which mostly pre-dates 5 ka, although fluvial deposits are detected in the Ghaggar palaeochannel at 3.8 ka and 3.0 ka, post-dating the decline of urbanism. Aeolian accumulation phases occur around 9 ka, 6.5 ka, 2.8 ka and 1.7 ka. There is no clear link to a 4.2 ka abrupt climate event, nor is there a simple switch between dominant fluvial deposition and aeolian accumulation, and instead the OSL ages reported present a view of a highly dynamic geomorphic system during the Holocene. The decline of Indus urbanism was not spatially or temporally instantaneous, and this paper suggests that the same can be said for the geomorphic response of the northern Thar to regional climate change.

Keywords Indus Civilisation, fluvial, aeolian, OSL dating, palaeoenvironment, drylands, northern Thar Desert

1. Introduction

A range of evidence suggests that the Holocene in the South Asian sub-continent experienced a series of arid-humid alterations on centennial and millennial scales (e.g. Gupta et al., 2003; Morrill et al., 2003; Berkelhammer et al. 2013; Dixit et al., 2014a), along with shorter, more abrupt events (e.g. Bond et al., 1997; Cullen et al., 2000). These fluctuations are set against a backdrop of an insolation-driven weakening of the Asian Monsoon (e.g. Berger and Loutre, 1999; Wang et al., 2005), which would have resulted in periods of variable precipitation and the onset of enhanced regional aridity. Holocene palaeohydrological records indicate how the Thar Desert landscape responded to variable climatic conditions, with data derived from southern Thar fluvial (Jain and Tandon, 2003; Jain et al., 2004; Thomas et al., 2007) and lacustrine systems (Singh, 1971; Singh et al., 1972, 1973, 1974, 1990; Bryson and Swain, 1981; Wasson et

al., 1984; Prasad et al., 1997; Enzel et al., 1999; Dixit et al., 2014a, 2014b). Regionally, these terrestrial palaeohydrological records suggest a period of greater water availability in the landscape during the early to mid-Holocene (~8 – 5 ka), leading to higher freshwater lake levels in Rajasthan and enhanced fluvial activity in the southern Thar (Jain and Tandon, 2003; Jain et al., 2004; Thomas et al., 2007). The period after ~5 ka appears to become increasingly arid, with falling lake levels and subsequent desiccation and a reduction and cessation of fluvial activity (e.g. Madella and Fuller 2006). There are now a number of high-resolution palaeoclimate proxy records that show variability in climatic conditions in the early to mid-Holocene, culminating in a period of drought around ~4 ka. Staubwasser et al. (2003) reconstructed Indus River discharge using the $\delta^{18}O$ signal from foraminifera found within delta sediments and observe variable output throughout the Holocene, with a significant drought phase centred around 4.2 kyr BP, which is followed by the establishment of a period of drought phases. Berkelhammer et al. (2012) analysed the $\delta^{18}O$ signal from a calcitic stalagmite found in Mawmulah Cave (northwest India) and identify a drought event, extreme in amplitude and duration, at 4.0 ka, with peak isotopic enrichment between 4.07 ± 0.02 and 3.89 ± 0.02 ka. This event also appears to be recorded in lacustrine deposits in Kotla Dahar lake, which document a sharp decline in lake level and hence monsoon intensity at a similar time (Dixit et al., 2014a). This widespread, regional mid-Holocene climatic deterioration would certainly have affected fluvial regimes on the plains of northwest India that were occupied during this period, and it is this that provides a testable hypothesis for establishing the relationship between climate, environment and society.

The Indus and Punjab alluvial plains that stretch across much of Pakistan and northwest India were first occupied during the mid-Holocene (e.g. Kenoyer, 1998; Possehl, 2002; Wright, 2010, Petrie et al. 2010) and the urban phase of the Bronze Age Indus Civilisation flourished across much of this area between 4.5 and 3.9 ka. The Indus was one of the most extensive complex societies in the pre-industrial world (e.g. Possehl, 2002; Wright, 2010), which was contemporaneous with the Akkadian, Egyptian and Chinese Neolithic, and is associated with the building of large cities such as Mohenjo-Daro, Harappa and Rakhigarhi, which housed tens of thousands of residents (Kenoyer, 1998), as well substantial numbers of smaller sites (Figure 1). After ~4 ka, all but one of the large Indus urban centres appear to have reduced in size and/or been abandoned, and there appears to have been a displacement of settlement towards the east, along the precipitation gradient towards the headwaters of the Yamuna and Sutlej River systems and towards Gujarat in northwest India (e.g. Petrie et al., 2017). The cause(s) influencing the demise or transformation of the urban centres has been the subject of discussion since Marshall's announcement of the discovery of the Indus Civilisation in the Illustrated London News in 1924. Socio-economic factors including economic depression, societal breakdown and invasion have all been proposed, along with environmental factors such as degradation, tectonic activity and climatic variability. These arguments have recently been summarised by Wright (2010) and Petrie et al. (2017).

In addition to the Indus River and its major tributaries, the Indus region is traversed by a palaeochannel known as the Hakra in Pakistan and the Ghaggar in India (hereon referred to as the Ghaggar-Hakra). This palaeochannel, the subject of investigation since the late nineteenth century (Mughal, 1997), has been described as a key river system for the Indus Civilisation (Kenoyer, 1998; Wright, 2010), and is associated with apparently one of the densest concentrations of related settlements in the Cholistan region (Mughal, 1997; Wright et al., 2008). That this now-ephemeral river channel was a focus of Indus settlement has meant that the link between fluvial activity in this system and urban collapse/demise has been discussed intensively (e.g. Stein, 1942; Wilhelmy, 1969; Gupta, 1996; Mughal, 1997; Chakrabarti and Saini, 2009; Gangal et al., 2010; Giosan et al., 2012). However, Wright (2010) and Petrie (2013) have emphasised that there are substantial gaps in geochronological evidence, both climatic and environmental, which hinders identification of a clear link between changes in climate, environment and society.

This study provides new chronological data relating to sedimentary units within this landscape system. We present new optically stimulated luminescence (OSL) ages for both fluvial and aeolian deposits spatially related with the Ghaggar-Hakra palaeochannel in northwest India and use these ages to infer landscape change during the Holocene. These ages are then linked to investigations from both northwest India and eastern Pakistan to provide a picture of changing Indus landscapes at the northern margin of the Thar Desert during the Holocene.

2. Regional setting and study framework

The Ghaggar-Hakra palaeochannel, traversing the northern margin of the Thar Desert in north-west India and eastern Pakistan, is part of a complex channel system on the Indo-Gangetic plains in NW India and Pakistan. Much of this forms a buried fluvial system and appears to pre-date the Indus Civilisation (e.g. Sinha et al., 2013; Mehdi et al., 2016; Singh et al., 2016). Its precise source is debated. In contrast to the other larger, higher energy Punjabi tributaries of the Indus (e.g. the Chenab, Ravi, Beas and Sutlej Rivers), the present day Ghaggar-Hakra river is relatively a much smaller fluvial system, which experiences ephemeral flow in response to monsoonal precipitation.

The region typically receives 80% of its annual precipitation from the Indian summer monsoon, with a steep NE-SW rainfall gradient across northwest India (Prasad and Enzel, 2006; Dixit et al. 2014a). The mean annual precipitation of ~690 mm in the northern Indo-Gangetic plains contrasts with ~100 mm in the Cholistan Desert in Pakistan (Sinha et al., 2013; Petrie et al., 2017). Studies of the Ghaggar-Hakra system have tended to focus on mapping from remotely sensed imagery (e.g. Ghose et al., 1979; Yash Pal et al., 1980; Sood and Sahai, 1983; Sahai, 1999; Radhakrishna and Merh, 1999; Gupta et al., 2004). Corroboration of these interpretations thorough field-based sedimentological and geomorphological investigation has only rarely been undertaken (e.g. Mehdi et al. 2016), yet this is important given the low gradients of the plain and temporal changes in channel behaviour and flow that could affect interpretations of past channel configurations and linkages.

More crucially, there are relatively few detailed sedimentological and geochronological analyses of the Ghaggar-Hakra palaeochannel and surrounding geomorphology. Singh et al. (2016) noted that palaeoenvironmental reconstructions using fluvial archives in this region have been limited, possibly due to the relative incompleteness of fluvial stratigraphic records (e.g. Jain et al., 2004). Only Giosan et al. (2012) have examined Ghaggar-Hakra sediments where it extends into Pakistan, focusing on a 200 km transect between Fort Abbas and Fort Derawar in the state of Punjab. There are more studies from the Indian sector, with Saini et al (2009) and Saini and Mutjaba (2010) providing mid-Holocene OSL ages for a tributary of the Ghaggar-Hakra in Haryana. Shitaoka et al. (2012; also Maemoku et al., 2012) focused primarily on aeolian dunes adjacent to the palaeochannel, reporting late Pleistocene/early Holocene aeolian accumulation in Rajasthan, which they conclude was subdued by insolation driven intensification of the monsoon system after ~9 ka.

3. Materials and Methods

We focus on a ~125 km west to east transect following the Ghaggar-Hakra between Suratgarh and Sirsa in an area where a large number of Indus Civilisation settlement sites have been found, including the large town site of Kalibangan in Rajastan. The area adjacent to the palaeochannel was targeted and after analysis of satellite imagery, eleven sites (Figure 2) with exposures of aeolian and fluvial sedimentary units (Figure

3) were identified and sampled for OSL dating. Units interpreted as fluvial in origin were sampled from five of the eleven sites. Sediments at these sites were typically fine sands and contained features such as rip up clasts or horizontal bedding structures, which confirmed them as low-energy fluvial deposits. The other six sites were dune sites closely associated with the palaeochannel, and these were sampled to ascertain the timing of aeolian phases. These dune sands tended to be slightly coarser in nature, and were deposited as massive units or had cross bedding structures preserved. Grain size analysis was undertaken using a Malvern Mastersizer Hydro 2000MU, and particle size ranges were determined from samples which had been oven dried. Data are summarised in Table 1.

Samples for OSL dating were collected by hammering opaque tubes into the sediment stratigraphy, which were subsequently removed, packed, and transported to the Oxford Luminescence Dating Laboratory. Samples were opened and prepared in subdued orange light conditions and the light-exposed sample ends were removed and sediments were treated with hydrochloric acid and hydrogen peroxide to remove carbonates and organic matter respectively, before sediment sieving and heavy liquid density separation to isolate the quartz mineral component. The resulting material was etched using hydrofluoric acid to remove the alpha-irradiated outer surface of the quartz grains and remove any non-quartz minerals still present. OSL measurements were made using a Risø TL/OSL luminescence reader fitted with a 10 mW green (532 nm, Nd:YVO4) focussed laser for stimulation and samples were irradiated with a $^{90}Sr/^{90}Y$ beta source with a dose rate of approximately 4 Gy/min. Ultraviolet luminescence signals were detected through a bialkali photo multiplier tube fitted with 7.5 mm U340 filters. Equivalent dose (D_e) values were calculated from single-grains of quartz using the single-aliquot regenerative dose (SAR) protocol (Murray and Wintle, 2000; Wintle and Murray, 2006) and following combined pre-heat and dose recovery tests, a pre-heat of 220°C for 10 s and cut-heat of 160°C were selected for use in the SAR protocol. Luminescence was measured at 125°C for 1 s at 90% laser power and D_es were calculated from the signal measured during the first 0.05 s of stimulation, with the mean background over the last 0.2 s subtracted. Luminescence signals were screened using a standard suite of rejection criteria, and only grains which satisfied the following were accepted for age calculation: i) recuperation of less than 5%; ii) recycling ratio within 10% of unity; iii) OSL IR depletion ratio (Duller, 2003) within 10% of unity; iv) test dose signal should be at least 3σ greater than background levels. Sample D_e determinations were made using the central age model (CAM) of Galbraith et al. (1999). Environmental dose rates were calculated from radionuclide concentrations measured using inductively coupled plasma mass spectrometry, which were converted to dose rates using the attenuation factors of Guerin et al. (2011). The infinite-matrix dose rates were adjusted for attenuation by grain size, chemical etching and a moisture content of 5 ± 2 %. All dose rates were calculated using the DRAC (v1.2) software of Durcan et al. (2015), available at ww.aber.ac.uk/alrl/drac and are summarised in Table 2.

Table 1: Particle size data according to grain-size class.

Sample (IND-)	% Very coarse to medium sand (2000–250 μm)	% Fine sand (250–125 μm)	% Very fine sand (125–63μm)	% Very coarse to coarse silt (63–16 μm)	% Medium to fine silt (16–4 μm)	% Very fine silt (4–2 μm)	% Clay (<2 μm)	% Total sand	% Total silt	% Total clay
Fluvial sediments										
14-4-1	2.14	28.12	19.35	31.90	11.58	3.71	3.20	49.61	47.19	3.20
14-4-2	3.70	24.78	18.84	33.87	16.81	1.28	0.72	47.32	51.96	0.72
14-6-1	0.48	0.68	5.20	52.71	33.51	4.71	2.71	6.36	90.93	2.71
14-6-2	0.03	0.64	3.15	45.07	38.31	6.16	6.63	3.82	89.55	6.63
14-7-1	11.81	39.92	21.05	10.98	10.40	2.54	3.30	72.77	23.93	3.30
14-7-2	14.01	47.75	21.83	12.47	2.97	0.77	0.20	83.59	16.21	0.20
14-7-3	5.80	21.12	20.27	38.08	9.80	3.68	1.25	47.19	51.56	1.25

14-8-1	4.15	26.87	21.47	24.89	15.17	3.34	4.11	52.49	43.40	4.11
14-8-2	3.94	33.48	21.26	18.72	16.97	3.17	2.46	58.68	38.86	2.46
14-9-1	4.60	35.81	26.58	16.23	11.02	2.34	3.42	66.99	29.59	3.42
14-9-2	3.59	29.06	24.29	23.64	13.37	2.40	3.63	56.95	39.42	3.63
Aeolian sediments										
14-1-1	12.66	41.15	22.73	9.95	8.11	2.37	3.04	76.54	20.43	3.04
14-1-2	17.81	46.12	29.26	2.17	3.98	0.52	0.14	93.19	6.67	0.14
14-1-3	14.67	52.89	27.12	2.13	1.98	0.52	0.69	94.68	4.63	0.69
14-2-1	24.81	56.09	18.38	0.72	0.00	0.00	0.00	99.28	0.72	0.00
15-7-1	1.86	49.09	39.62	3.96	3.48	0.84	1.15	90.57	8.28	1.15
15-7-4	3.80	53.31	39.80	3.08	0.00	0.00	0.00	96.92	3.08	0.00
15-8-1	12.92	42.31	36.74	3.92	3.57	0.54	0.00	91.97	8.03	0.00
15-8-4	9.73	38.78	45.37	2.26	2.02	1.31	0.53	93.88	5.59	0.53
15-9-1	10.27	46.45	37.64	2.08	1.96	1.00	0.60	94.36	5.04	0.60
15-9-2	13.07	42.12	38.21	2.43	2.16	1.23	0.78	93.40	5.82	0.78
15-10-1	12.22	53.69	28.58	3.79	0.99	0.30	0.43	94.49	5.08	0.43
15-10-2	10.27	52.29	31.29	3.60	2.10	0.40	0.05	93.85	6.10	0.05
15-10-3	11.36	48.55	34.50	2.84	1.87	0.86	0.02	94.41	5.57	0.02

Table 2: Equivalent dose (D_e), dose rate ($\dot{D}$) and OSL age summary. Equivalent doses, dose rates, and ages are shown to two decimal places, with all calculations made prior to rounding.

Sample (IND-)	Depth (m)	Grain size (μm)	# Grains measured (accepted)	Over-dispersion (%)	CAM D_e (Gy)	Beta $\dot{D}$ (Gy.ka^{-1})	Gamma $\dot{D}$ (Gy.ka^{-1})	Cosmic $\dot{D}$ (Gy.ka^{-1})	Environmental $\dot{D}$ (Gy.ka^{-1})	Age (ka)
Fluvial samples										
14-4-1	0.8	150-210	1600 (45)	33.5 ± 1.7	8.61 ± 1.26	1.54 ± 0.12	1.10 ± 0.07	0.18 ± 0.02	2.82 ± 0.14	3.05 ± 0.47
14-4-2	1.5	150-210	1900 (46)	33.5 ± 2.5	10.67 ± 1.19	1.54 ± 0.12	1.09 ± 0.07	0.17 ± 0.02	2.80 ± 0.13	3.81 ± 0.46
14-6-1	0.5	90-250	900 (24)	29.1 ± 2.4	2.61 ± 0.32	1.96 ± 0.16	1.32 ± 0.08	0.20 ± 0.02	3.48 ± 0.18	0.75 ± 0.10
14-6-2	1.5	90-250	700 (23)	47.7 ± 3.5	13.03 ± 2.90	2.55 ± 0.21	1.79 ± 0.12	0.17 ± 0.02	4.51 ± 0.24	2.89 ± 0.66
14-7-1	0.5	150-210	2200 (64)	41.1 ± 3.2	16.38 ± 2.16	1.81 ± 0.15	1.19 ± 0.08	0.20 ± 0.02	3.20 ± 0.17	5.12 ± 0.73
14-7-2	1.5	150-210	2600 (60)	38.6 ± 2.6	17.54 ± 2.10	1.44 ± 0.12	0.97 ± 0.06	0.17 ± 0.02	2.58 ± 0.13	6.79 ± 0.89
14-7-3	3.5	150-210	2600 (68)	35.6 ± 2.9	19.70 ± 2.08	1.28 ± 0.10	0.89 ± 0.06	0.13 ± 0.01	2.30 ± 0.12	8.57 ± 1.01
14-8-1	1.8	150-210	1900 (47)	35.5 ± 4.1	14.21 ± 1.89	1.97 ± 0.15	1.48 ± 0.10	0.16 ± 0.02	3.62 ± 0.18	3.93 ± 0.56
14-8-2	2.8	150-210	2000 (52)	32.7 ± 2.8	20.99 ± 2.11	1.81 ± 0.14	1.35 ± 0.09	0.15 ± 0.01	3.30 ± 0.17	6.36 ± 0.72
14-9-1	0.6	150-210	2000 (53)	29.1 ± 2.5	7.18 ± 0.97	1.95 ± 0.16	1.29 ± 0.08	0.20 ± 0.02	3.44 ± 0.18	2.09 ± 0.30
14-9-2	1.25	150-210	1800 (49)	42.7 ± 4.7	23.02 ± 3.01	2.02 ± 0.16	1.32 ± 0.09	0.18 ± 0.02	3.52 ± 0.19	6.54 ± 0.93
Aeolian samples										
14-1-1	0.5	180-210	1700 (67)	39.3 ± 2.9	5.37 ± 0.86	1.65 ± 0.12	1.32 ± 0.09	0.20 ± 0.02	3.17 ± 0.15	1.69 ± 0.28
14-1-2	1.0	180-210	1900 (58)	48.6 ± 2.3	8.01 ± 0.61	1.62 ± 0.12	1.23 ± 0.08	0.18 ± 0.02	3.02 ± 0.15	2.65 ± 0.24
14-1-3	2.2	180-210	2600 (49)	38.4 ± 2.2	8.53 ± 0.96	1.63 ± 0.13	1.17 ± 0.08	0.16 ± 0.02	2.95 ± 0.15	2.89 ± 0.36
14-2-1	1.0	180-210	2200 (48)	51.2 ± 4.0	0.61 ± 0.10	1.43 ± 0.11	0.98 ± 0.06	0.18 ± 0.02	2.60 ± 0.13	0.23 ± 0.04
15-7-1	0.5	180-210	1700 (47)	29.5 ± 2.0	24.70 ± 2.94	1.40 ± 0.10	1.17 ± 0.08	0.21 ± 0.02	2.77 ± 0.13	8.93 ± 1.14
15-7-4	3.3	180-210	2100 (53)	31.4 ± 2.7	20.58 ± 1.75	1.27 ± 0.10	0.91 ± 0.06	0.14 ± 0.01	2.32 ± 0.12	8.89 ± 0.88
15-8-1	0.5	180-210	2600 (61)	41.6 ± 3.6	0.31 ± 0.10	1.27 ± 0.10	0.99 ± 0.07	0.20 ± 0.02	2.46 ± 0.12	0.12 ± 0.04
15-8-4	2.0	180-210	2500 (68)	48.9 ± 3.4	17.33 ± 1.90	1.34 ± 0.11	0.95 ± 0.06	0.16 ± 0.02	2.46 ± 0.13	7.06 ± 0.85
15-9-1	3.0	180-210	2300 (62)	38.0 ± 2.9	15.82 ± 1.39	1.35 ± 0.11	0.97 ± 0.06	0.11 ± 0.01	2.44 ± 0.13	6.49 ± 0.66
15-9-2	4.9	180-210	2200 (55)	36.3 ± 2.4	16.06 ± 1.13	1.19 ± 0.09	0.92 ± 0.06	0.14 ± 0.01	2.25 ± 0.11	7.13 ± 0.61

15-10-1	0.6	180-210	2000 (49)	44.3 ± 4.0	5.46 ± 0.38	1.32 ± 0.10	0.97 ± 0.07	0.20 ± 0.02	2.49 ± 0.12	2.20 ± 0.19
15-10-2	1.4	180-210	2400 (51)	31.6 ± 2.4	12.38 ± 0.99	1.43 ± 0.11	1.12 ± 0.08	0.17 ± 0.02	2.73 ± 0.13	4.54 ± 0.43
15-10-3	2.4	180-210	2500 (63)	35.3 ± 3.1	14.28 ± 0.49	1.34 ± 0.11	0.99 ± 0.07	0.15 ± 0.02	2.48 ± 0.12	5.76 ± 0.35

4. Results

Particle size data are presented in Table 1 and Figure 4. With the exception of sample IND-14-1-1, which has a slightly larger silt component, the aeolian samples comprise at least 90% sand sized particles (<63 μm) (Table 1), highlighted in the grain size profiles of selected samples in Figure 4a. The suite of fluvial samples are more variable in composition, on average comprising 49% sand but with individual values ranging between ~4 and 84 % (Table 1). The grain size profiles in Figure 5b illustrate the increased clay and silt components, particularly for sample IND-14-6-2, where 96% of grains are smaller than 63 μm, hence the difficulty extracting adequate sediment mass for OSL dating (below). Volumetric proportions of clay, silt and sand sized particles aside, the majority of samples have dominant peaks in sand at around 100 to 120 μm and silt between 15 and 30 μm (Figure 5), and this may suggest an element of reworking of sediments on the floodplain.

Single grain OSL ages are shown in Table 2 and Figure 2. For the majority of samples between 1700 and 2600 grains were measured for D_e determination, however the fine nature of sediments from site IND-14-6 only provided enough sand sized sediment for 700 – 900 grains to be measured. The number of grains providing a luminescence signal discernible from background levels (e.g. Figure 5a) and satisfying the rejection criteria varied between 1.8% and 3.9%. At least 45 accepted luminescence signals were used for sample D_e determination for all samples, apart from samples IND-14-6-1 and IND-14-6-2, where a lack of sand sized material meant fewer grains could be measured and screened. Dose recovery tests on samples IND-14-1-1, IND-14-7-2 and IND-15-9-1 provided recovery ratios of 0.93 ± 0.06, 0.97 ± 0.09, and 0.94 ± 0.09 respectively, indicating that the SAR protocol and selected measurement and analysis parameters used for D_e determination can successfully recover an applied laboratory dose. Analyses of luminescence signals from small aliquots of sample suggest signals are dominated by the fast component in the initial part of the OSL signal (e.g. Durcan and Duller, 2011).

Overdispersion (σ_d), or the heterogeneity in D_e distributions beyond that which would be expected from uncertainties arising from intrinsic luminescence properties alone, is moderately high for this suite of samples, ranging between 29.1 and 51.2 %, although there is no systematic difference between sediments which were deposited by aeolian and fluvial depositional processes. σ_d in dose distributions may originate from a multitude of factors, either in isolation or combination, including heterogeneous bleaching (e.g. Jain et al., 2004; Olley et al., 2004), environmental dose rate heterogeneity (e.g. Nathan et al., 2003) and post-depositional sediment mixing (e.g. Bateman et al., 2007; Kristensen et al., 2015). None of the analysed samples display characteristics of incomplete bleaching, e.g. a sharp leading edge of lower D_e values, with a scatter of higher D_es (Jain et al., 2004; Lyons et al., 2014). Instead, whilst dispersed, values tend to cluster around a central value, and factors other than incomplete bleaching are hypothesised to drive variability in D_e distributions. Therefore, CAM has been used for D_e calculation (Galbraith et al., 1999), following the rationale of other studies including Rowan et al. (2012), Parton et al. (2015) and Duller et al. (2015), where observed dose distributions in a range of geomorphic settings are simultaneously highly overdispersed but display symmetricity around a central D_e value (e.g. Figure 5b).

Of the five fluvial sites dated, sites IND-14-4 and IND-14-6 are located in the main Ghaggar-Hakra palaeochannel identified in satellite imagery (Figure 2). Two samples for OSL dating were taken from site

IND-14-4 near Suratgarh, and at this site the silty-sands sampled (Table 1) for OSL dating dates fluvial deposition to the mid-Holocene at this site, at 3.05 ± 0.47 ka and 3.81 ± 0.46 ka. The 0.75 m of sediments above sample IND-14-4-1 were not sampled because in-field assessment suggested a high proportion of silt and clay sized particles with little sand, which would not have yielded sufficient sand for coarse grain OSL dating. These sediments were finely horizontally laminated and contained small carbonate nodules. Further west, fluvial sediments from the channel adjacent to the Indus settlement of Kalibangan were sampled (site IND-14-6). Again sediments are extremely fine-grained, predominantly clays and silts (Table 1). Even when using an extended grain size range for OSL dating (90 – 250 um), very few sand grains were extracted for coarse grain dating and these OSL ages should be considered as very small aliquot rather than single grain ages. Nonetheless, 1.5 m below the surface of the current channel, fluvial deposition is recorded at 2.89 ± 0.66 ka, correlating well with the upper age of 3.05 ± 0.47 ka at IND-14-4. Deposits from the upper part of site IND-14-6, from a section of the Ghaggar-Hakra adjacent to Kalibangan, demonstrate more recent fluvial deposition, with an OSL age of 0.75 ± 0.10 ka, although the extremely fine-grained nature of sediments recorded (Table 1, Figure 5b) does not suggest deposition under intensive fluvial conditions, but rather low energy, possibly ephemeral flooding or ponding.

Three sites, IND-14-7, IND-14-8 and IND-14-9, were sampled along the tributary to the south of the main Ghaggar-Hakra palaeochannel and to the east of Kalibangan,. Early to mid-Holocene ages are recorded at the base of the three sequences: 8.57 ± 1.01 ka, 6.36 ± 0.77 ka and 6.54 ± 0.93 ka respectively (Table 2, Figure 2). Deposition of fluvial sands continued until ~5 ka at IND-14-7 and ~3.9 ka at IND-14-8. This represents the uppermost part of the sequence at IND-14-7, although there is approximately 1.5 m of fine clayey-silts preserved at IND-14-8. These ages correspond with OSL dates presented by Saini and Mutjaba (2010) who sampled two sites from the same channel approximately 100 km further to the east. They reported OSL ages of 5.9 ± 0.3, 5.6 ± 0.2, 4.3 ± 0.2 ka, 3.4 ± 0.2 ka, 3.0 ± 0.2 ka and 2.9 ± 0.2 ka for what they describe as silty fluvial sands, which are capped with laminated clays post 3 ka. OSL ages calculated in this study for this southern tributary are in line with the older ages published by Saini and Mutjaba (2010), although the fluvial deposits dated in this study tend to be older. This may be due to differences in sampling strategy or sediment preservation, but may also reflect system avulsion and spatially discontinuous channel abandonment across the Ghaggar-Hakra plain. Investigating the stratigraphy of fluvial deposition from deep cores across a transect of the Ghaggar-Hakra plain at Kalibangan, Sinha et al. (2013) find evidence for an earlier braided fluvial system, which subsequently evolves into a channelised system, many channels of which are now buried. Detailed sedimentological analysis of these cores shows medium to coarse sand units deposited under high energy fluvial conditions overlain by finer fluvial sands deposited under a lower energy regime (Singh et al., 2016).

OSL dating of the aeolian deposits suggests aeolian accumulation throughout the Holocene. Ages at sites IND-14-1 and IND-14-2 indicate aeolian deposition from 2.89 ± 0.36 ka, post-dating fluvial activity at ~3.0 ka in the Ghaggar-Hakra palaeochannel at site IND-14-4 (OSL age 3.05 ± 0.47 for sample IND-14-4-1), 1 km to the east. Aeolian accumulation appears to have been preserved in two phases; one at ~1.7 ka (IND-14-1-1) and the other between 2.65 and 2.9 ka (IND-14-1-2 and -14-1-3). Late Holocene aeolian accumulation is also seen in the upper part of site IND-15-10, with an OSL age of 2.20 ± 0.19 ka. At sites slightly to the west (IND-15-8, -15-9 and -15-10), older aeolian sediments have been preserved, with OSL ages ranging between 4.54 ± 0.43 ka (sample IND-15-10-2) and 7.13 ± 0.61 ka (IND-15-9-2). At the eastern extent of the study area at site IND-15-7, close to the town of Sirsa, the oldest OSL ages in this study are recorded. At this site, two OSL ages of 8.93 ± 1.14 ka (from 0.5 m below the current land surface) and 8.89 ± 0.88 ka (3.3 m) suggest accumulation within the same aeolian phase (within the level of uncertainty associated with the OSL dating). These ages are more or less in line with those presented by Shitaoka et al. (2012) and Maemoku et

al. (2012) who dated aeolian deposits bordering the Ghaggar-Hakra palaeochannel. In their studies, dune deposits pre-date 4.9 ± 0.3 ka at all of their sites, and they report accumulation at around 5 ka and between 10 - 15 ka.

5. Discussion

5.1 Holocene landscape dynamics on the Ghaggar-Hakra interfluve

This suite of OSL ages presents a view into a dynamic Holocene environment at the northern margin of the Thar Desert. The chronology of Holocene fluvial and aeolian sedimentation presented here complements other records of regional geomorphological and environmental change in northwest India. Further upstream in the Ghaggar-Hakra, Saini et al. (2009) and Saini and Mutjaba (2010) reported fine-grained fluvial deposition between 6 and 4.3 ka, after which an upward fining of sediments is interpreted as representing a decline in fluvial competence (Saini et al., 2009), culminating in channel abandonment at 3.4 ka (Saini and Mutjaba, 2010). Particle size analysis of the sediments dated in this study does not show a significant change in particle size with age, although the majority of fluvial samples have a greater relative proportion of silt and clay sized material. At sites such as IND-14-4 and IND-14-8 (Figure 1), upper sediment units were not sampled as field assessment pointed towards insufficient sand for OSL dating, and this, along with the measured fine-grained nature of the fluvial samples taken from across the Ghaggar-Hakra interfluve is consistent with Saini and Mutjaba's (2010) study. In the main Ghaggar-Hakra palaeochannel at site 14-6, sample IND-14-6-2 indicates a phase of fluvial deposition at at c.2.9 ka. This sample consisted of at least 93% silt and clay (Table 1, Figure 4b), and he extremely fine-grained nature of these sediments suggests extremely low-energy fluvial conditions for the deposition of these sediments. At around the same time, dune accumulation on the interfluve is recorded at site IND-14-1.

Few Holocene fluvial records from the Thar have been published, and regional studies have tended to focus on either broader late Quaternary reconstructions (e.g. Srivastava et al., 2001; Juyal et al., 2006; Juyal et al., 2009; Singhvi et al., 2010) or the historical period (e.g. Thomas et al., 2007; Kunz et al., 2010; Jayangondaperumal et al., 2012). That said, early to mid-Holocene fluvial activity (12 – 5 ka) has been noted in the now ephemeral Luni River system, south Rajasthan (Jain et al., 2004), and strengthened flow in the perennial Mahi and Sabarmati systems in Gujurat is also reported for this period (Jain and Tandon, 2003; Tandon et al.,1997). These broad trends for enhanced early Holocene fluvial activity, as well as increased aeolian accumulation after ~5 ka in the semi-arid Thar are also seen in the area around Ghaggar-Hakra palaeochannel in both India and Pakistan (e.g. Giosan et al., 2012).

Aeolian accumulation is recorded across the study area. Within the past 100 – 200 years, there a phase of accumulation/reactivation has been sampled. Accumulation is also recorded at a number of sites between ~7.1 – 5.7 ka and ~ 2.9 – 1.7 ka. In addition, one age of 4.54 ± 0.43 ka (IND-15-10) to the west and the accumulation of ~2.5 m of sands at IND-15-7 at ~8.9 ka (8.93 ± 1.14 and 8.89 ± 0.88 ka) to the east have been identified. Records of aeolian accumulation in the Thar tend to be spatially and temporally discontinuous. Singhvi and Kar (2004) suggest a Holocene aeolian history which sees Monsoon winds drive aeolian activity until ~7 ka, followed by a phase of subdued accumulation between 7 and 6 ka, due to more intense precipitation. Aeolian aggradation between ~5 ka – 3.5 ka, based on records from the Jaisalmer region (Kar et al., 1998) and in Rajasthan (Thomas et al., 1999) is inferred, although Singhvi and Kar (2004) comment that there is little regional trace of this aridity phase. They suggest that there is a lull in activity between ~3.7 – 2.0 ka, which is followed by a period of more intensive aeolian activity. The geochronology presented in this study suggests aeolian accumulation continues for longer during the mid- Holocene until

5.7 ka and is recorded again from ~2.9 ka. On the margin of the Thar and in association with the interfluve, dune activity in this area is likely sensitive to hydrological conditions (e.g. Thomas and Burrough, 2016), where the gradual drying of the fluvial system will increase sediment availability for deflation, alongside the preservation potential of aeolian sediments on the interfluve.

It is clear from our OSL ages (Table 1; Figure 6) that fluvial deposition and aeolian accumulation occur concurrently. Dune accumulation on and adjacent to the Ghaggar-Hakra interfluve occurs during phases of low energy fluvial deposition within the palaeochannel, particularly around ~6.5 ka and ~2.8 ka. From the grain size profiles in figure 4, whilst the relative abundance of sand and silt differs between the fluvial and aeolian samples, peaks in fine sand of ~100 μm and silt at ~20 μm occur in both sets of samples. It is therefore hypothesised that interfluve sediments are reworked into dune deposits during periods of relatively increased aridity, when more limited moisture levels provide increased sediment for entrainment. The interaction of aeolian and hydrological activity suggests a climatic oscillation between periods of enhanced and subdued humidity.

5.2 The Ghaggar-Hakra within a regional context of environmental change

Dry and ephemeral lake systems are important sources of environmental change data in the region. Since the studies of Singh (1971) and Singh et al. (1972, 1973, 1974) investigations of lake deposits at Lunkaransar (Bryson and Swain, 1981; Enzel et al., 1999), Didwana (Bryson and Swain, 1981; Wasson et al., 1984), Nal Sarovar (Prasad et al., 1997) and more recently Riwasa (Dixit et al., 2014b) and Kotla Dahar (Dixit et al., 2014a) have added to the reconstruction of palaeoenvironment and climate in the northwest of India. At palaeolake Kotla Dahar, Haryana, Dixit et al. (2014a) document a relatively deep fresh water lake between 6.5 and 5.8 ka, with progressive lowering of the lake (and increased salinity) after 5.8 ka. The disappearance of ostracods and a rapid increase in the $\delta^{18}O$ of gastropods at ~4.1 ka is interpreted as the onset of an intense arid event with a duration of up to 200 years before a return to more 'normal' conditions. Dixit et al. (2014a) draw parallels with a similar drying event recorded in the Mawmulah Cave speleothem in northeast India (Berkelhammer et al., 2012). In contrast, at Lake Riwasa, the $\delta^{18}O$ signal from lake ostracods suggests a drying trend between 6.8 – 6.5 ka. At Lake Didwana, Singh et al. (1990) reported falling lake levels between ~6 – 4.5 ka, with Enzel et al. (1999) proposing a drying phase from approximately 5 ka, with a switch from a perennial water body to a playa/episodic lake at ~4.7 ka. Whilst these reconstructions may reflect local conditions, with climate being only one driving factor, higher lake levels and palaeo-precipitation is inferred during the early and mid-Holocene at Lakes Didwana, Lunkaransar and Kotla Dahar. These periods of more intensive fluvial deposition correspond well with the OSL ages in the Ghaggar-Hakra palaeochannel presented in this study. Fluvial deposition in the Ghaggar-Hakra channel extends beyond the arid events seen in the high resolution records of Berkelhammer et al. (2012) and Dixit et al. (2014a, 2014b), and this presents a number of hypotheses. It is possible that this deposition indicates continued fluvial activity during the arid events observed in the Mawmulah and Kotla Dahar records, or perhaps a return to more normal conditions after the intense aridity event (e.g. Figure 6b). The 1 sigma uncertainties associated with the OSL ages do not provide the resolution to allow this to be investigated fully at this stage. That dune building occurs at the same time as fluvial deposition during the Holocene reflects a not uncommon landscape state in drylands (e.g. Thomas, 2013), where changing hydrological conditions can provide increased sediment availability and the potential for aeolian accumulation. It could be suggested that the early to mid-Holocene ages for aeolian accumulation with the Mawmulah speleothem coincided with higher $\delta^{18}O$ values (lower precipitation) (Figure 6). These phases of reduced precipitation may have provided enhanced landscape stability on the interfluve, thus allowing the deflation, deposition and preservation of floodplain sediments as aeolian geoproxies. However, the uncertainties

associated with the OSL ages exceed the duration of the oscillations observed in the Mawmulah record, and a firm conclusion cannot be made at present. However, in terms of the geomorphic behaviour of dryland environments, sediment availability and the coincidence of aeolian accumulation and fluvial activity provides a testable hypothesis to explain aeolian accumulation on the Ghaggar-Hakra interfluve during a period of relatively more intense Monsoon activity.

5.3 Changing landscapes and the Indus Civilisation

Hydrological changes in the Ghaggar-Hakra system and mid-Holocene climatic variability more generally have long been suggested as important for the decline of Indus urbanism by 3.9 ka (e.g. Singh, 1971; Singh et al., 1974; Mughal, 1997; Enzel et al., 1999; Prasad and Enzel, 2006; Staubwasser and Weiss, 2006; MacDonald, 2011; Giosan et al., 2012; Petrie et al., 2017). A gradual aridification of the Thar after 5.0 ka appears to have provided a window of opportunity where the fertile floodplains adjacent to the Ghaggar-Hakra palaeochannel were used for inundation agriculture (Singh et al., 2010; Singh et al., 2012; Petrie et al., 2017). Giosan et al. (2012, p. E1690) suggested that monsoon-driven channel flow in the Ghaggar-Hakra was perennial prior to 4.5ka, becoming ephemeral thereafter. The possibility that monsoon-driven precipitation was sufficient for perennial flow has, however, been questioned (Petrie, 2017). During the urban Indus phase, it has been speculated that Indus populations were utilising a system where flooding was regular and manageable, which Petrie et al. (2017) describe this as a system which would have been 'predictably unpredictable'. Regional archaeological records indicate that Indus populations occupied much of the Ghaggar-Hakra floodplain until ~3.9 ka (e.g. Joshi et al. 1984; Mughal 1997; Kumar 2009; Singh et al., 2010, 2011), after which settlement appears to have moved east towards areas which may have experienced more reliable rainfall (Madella and Fuller, 2006; Petrie et al., 2017).

Whilst regional climatic deterioration driven by the weakening of the Monsoon system would have seen increasing aridification of this area, our analysis demonstrates that at least part of the Ghaggar-Hakra was still flooding after the demise of the Indus urban centres. The dating results presented in this study focused on fluvial deposits preserved close to the modern surface, and it has been shown that the palaeochannel visible today is only one of a complex, multi-channel system (e.g. Sinha et al., 2013; Mehdi et al., 2016; Singh et al., 2016; Orengo and Petrie, 2017). Fluvial reorganisation and avulsion would have been likely as monsoon-derived precipitation became more variable throughout the Holocene. An assessment of the response of this fluvial system on a broader scale is required to understand how the Indus landscape would have changed during the urban phase. Indus populations occupied a diverse range of environmental and ecological zones (Possehl, 2002; Singh and Petrie, 2009; Weber et al., 2010; Wright, 2010; Petrie, 2013; Dixit et al., 2014a; Petrie et al., 2017, Petrie and Bates, 2017) and the decline of the Indus Civilisation did not occur instantaneously, temporally or spatially (Wright, 2010). As such, the proposition of climate change as the sole reason for urban collapse and/or transformation is clearly an oversimplification of a complex process that occurred over a prolonged period (Wright, 2010; Petrie 2017).

6. Conclusion

This study presents OSL ages for Holocene fluvial and aeolian activity in the Ghaggar-Hakra interfluve on the northern margin of the Thar Desert. This chronology shows fluvial deposition in the currently visible palaeochannel during the early Holocene from 8.5 ka until ~3 ka. More intensive fluvial processes are inferred prior to 5 ka, when thicker fluvial units are deposited. After 3 ka, sediments in the Ghaggar-Hakra channel at Kalibangan fine significantly, and slightly further to the west, sediment dated to 3 ka are capped by a silty unit of 0.75 m. This may suggest a weakening of fluvial activity post 3 ka and possibly ephemeral

overbank flooding in this area at least. These findings complement other studies in the Ghaggar-Hakra system (e.g. Saini et al., 2009, Saini and Mutjaba, 2010) and are consistent with regional palaeohydrological records (e.g. Dixit et al., 2014a, 2014b). Like the fluvial sedimentation, aeolian accumulation is recorded across the Holocene, with a period of enhanced accumulation at around 9 ka identified, as well as two ranges of ages at around ~7.1 – 5.7 ka and later between ~2 – 1.7 ka. These ages are consistent with regional records of aeolian accumulation in Ghaggar-Hakra region (e.g. Shitaoka et al., 2012) and more broadly in the Thar Desert (e.g. Kar et al., 1998; Thomas et al., 1999; Singhvi and Kar, 2004). In this study we demonstrate phases of fluvial activity and aeolian accumulation coincide, which should be considered as normal behaviour in a dryland context (Thomas, 2013).

This evidence adds to the emerging picture of the Holocene Ghaggar-Hakra as a low energy fluvial system broadly driven by regional changes in the monsoon, however, this response appears to be neither simple nor linear. Thicker units of fluvial sediment are deposited in the early Holocene, although in the sediments sampled, there is no statistically significant change in particle size which can be used to infer a weakening of fluvial transport energies with time. Thinner fluvial units accumulated during the mid-Holocene and the presence of fine sediments, predominantly silts, in the channel close to the Indus Civilisation urban site Kalibangan after 3 ka may represent a phase of weakened fluvial activity. Coeval fluvial and aeolian accumulation provides a view of oscillating phases of relative humidity and aridity throughout the Holocene, resulting in the accumulation of dune sediments on the Ghaggar-Hakra interfluve. Further research considering the geomorphic and environmental response to climatic fluctuation across the full extent of the Ghaggar-Hakra interfluve, which will further improve our understanding of changing environmental conditions under fluctuating monsoon regimes, as well as inform the response of past civilisations to climatic and environmental variability.

Acknowledgements

JAD and DSGT thank the John Fell Fund, University of Oxford for providing the funding which allowed this study to be undertaken. JAD thanks St John's College, Oxford for supporting attendance at the European Geosciences Union in 2016, where this work was initially presented. We thank the anonymous reviewer for their comments and suggestions.

References

Bateman, M.D., Boulter, C.H., Carr, A.S., Frederick, C.D., Peter, D., Wilder, M., 2007. Detecting post-depositional sediment disturbance in sandy deposits using optical luminescence. Quaternary Geochronology 2, 57-64.

Berger, A., Loutre, M.F., 1999. Parameters of the Earths orbit for the last 5 million years in 1 kyr resolution. doi:10.1594/PANGAEA.56040.

Berkelhammer, M., Sinha, A., Stott, L., Cheng, H., Pausata, F.S.R., Yoshimura, K., 2012. An abrupt shift in the Indian monsoon 4000 years ago. In Giosan, L., Fuller, D.Q., Nicoll, K., Flad, R.K., Clift, P.D. (eds.), Climates, landscapes, and civilizations: American Geophysical Union Geophysical Monograph 198, pp. 75– 87.

Bond, G., Showers, W., Cheseby, M., Lotti, R., Almasi, P., de Menocal, P., Priore, P., Cullen, H., Hajdas, I., Bonani, G., 1997. A pervasive millennial-scale cycle in North Atlantic Holocene and glacial climates. Science 278, 1257-1266.

Bryson, R.A., Swain, M.A., 1981. Holocene variations in monsoon rainfall in Rajasthan. Quaternary Research 16, 135-145.

Chakrabarti, D.K., Saini, S., 2009. The problem of the Sarasvati River and notes on the archaeological geography of Haryana and Indian Punjab. Aryan Books International, Delhi.

Cullen, H.M., de Menocal, P.B., Hemming, S., Hemming, G., Brown, F.H., Guilderson, T., Sirocko, F., 2000. Climate change and the collapse of the Akkadian empire. Evidence from the deep sea. Geology 28, 379-382.
Dixit Y., Hodell D.A., Petrie C.A., 2014a. Abrupt weakening of the summer monsoon in northwest India 4100 yr ago. Geology 42, 339-342.
Dixit, Y., Hodell, D.A., Petrie, C.A., Sinha, R., 2014b. Abrupt weakening of the Indian summer monsoon at 8.2 kyr BP. Earth and Planetary Science Letters, 391, 16-23.
Duller, G.A.T., 2003. Distinguishing quartz and feldspar in single grain luminescence measurements. Radiation Measurements 37, 161-165.
Duller, G.A.T., Tooth, S., Barham, L., Tsukamoto, S., 2015. New investigations at Kalambo Falls Zambia: Luminescence chronology, site formation and archaeological significant. Journal of Human Evolution, 85, 111-125.
Durcan, J.A., Duller, G.A.T., 2011. The fast ratio: a rapid measure for testing the dominance of the fast component in the initial OSL signal from quartz. Radiation Measurements 46, 1065-1072.
Durcan, J.A., King, G.E., Duller, G.A.T., 2015. DRAC: Dose rate and age calculator for trapped charge dating. Quaternary Geochronology, 28, 54-61.
Enzel, Y., Ely, L., Misra, S., Ramesh, R., Amit, R., Lazar, B., Rajaguru, Baker, V.R., Sandler, A., 1999. High-resolution Holocene environmental changes in the Thar Desert, northwestern India. Science 284, 125-128.
Galbraith, R.F., Roberts, R.G., Laslett, G.M., Yoshida, H., Olley, J.M., 1999. Optical dating of single and multiple grains of quartz from Jinmium rock shelter, northern Australia: part I, experimental design and statistical models. Archaeometry 41, 339-364.
Gangal, K., Vahia, M., Adhikari, R., 2010. Spatio-temporal analysis of the Indus urbanisation. Current Science 98, 846-852.
Ghose, B., Kar, A., Hussain, Z., 1979. The lost courses of the Saraswati River in the Great Indian Desert: new evidence from Landsat Imagery. The Geographical Journal 145, 446-451.
Giosan, L., Clift, P.D., Macklin, M.G., Fuller, D.Q., Constantinescu, S., Durcan, J.A., Stevens, T., Duller, G.A.T., Tabrez, A., Gangal, K., Adhikari, R., Alizai, A., Filip, F., VanLaningham, S., Syvitski, J.P.M., 2012. Fluvial landscapes of the Harappan civilisation. Proceedings of the National Academy of Sciences of the United States of America, doi:10.1073/pnas.1112743109.
Guerin, G., Mercier, N., Adamiec, G., 2011. Dose-rate conversion factors: update. Ancient TL 29, 5-8.
Gupta, S.K., 1996. The Indus-Saraswati civilisation: origins, problems and issues. Pratibha Prakashan, Delhi.
Gupta, A.K., Anderson, D.M., Overpeck, J.T., 2003. Abrupt changes in the Asian southwest monsoon during the Holocene and their links to the North Atlantic Ocean. Nature 421, 354-357.
Gupta, A.K., Sharma, J.R., Sreenivasan, G., Srivastava, K.S., 2004. New findings on the course of River Saraswati. Journal of Indian Society of Remote Sensing 32, 1-24.
Jain, M., Tandon, S.K., 2003. Fluvial response to Late Quaternary climate changes, western India. Quaternary Science Reviews 22, 2223-2235.
Jain, M., Tandon, S.K., Bhatt, S.C., 2004. Late Quaternary stratigraphic development in the lower Luni, Mahi and Sabarmati river basins, western India. Proceedings of the Indian Academy of Science 113, 453-471.
Jayangondaperumal, R., Murari, M.K., Sivasubramanian, P., Chandresekar, N., Singhvi, A.K., 2012. Luminescence dating of fluvial and coastal red sediments in the SE coast, India, and implications for palaeoenvironmental changes and dune reddening. Quaternary Research 77, 468-481.
Joshi, J.P., Bala, P.M., Raj, J., 1984. The Indus Civilisation: A reconstruction on the basis of distribution maps. In: Lal BB and Gupta SP, eds., Frontiers of the Indus Civilisation. New Delhi, Books and Books, 511-539.
Juyal, N., Chamyal, L. S., Bhandari, S., Bhushan, R., Singhvi, A. K., 2006. Continental record of the southwest monsoon during the last 130 ka: evidence from the southern margin of the Thar Desert, India. Quaternary Science Reviews 25, 2632-2650.
Juyal, N., Pant, R.K., Basavaiah, N., Bhushan, R., Jain, M., Saini, N.K., Yadava, M.G., Singhvi, A.K., 2009. Reconstruction of Last Glacial to early Holocene monsoon variability from relict lake sediments of the Higher Central Himalaya, Uttrakhand, India. Journal of Asian Earth Science 34, 437-449.
Kar, A., Felix, C., Rajaguru, S.N. and Singhvi, A.K., 1998. Late Holocene growth and mobility of a transverse dune in the Thar desert. Journal of Arid Environments, 38, 175-185.
Kenoyer, J.M., 1998. Ancient cities of the Indus Valley Civilisation. Oxford University Press, Oxford.

Kristensen, J.A., Thomsen, K.J., Murray, A.S., Buylaert, J.-P., Jain, M., Breuning-Madsen, H., 2015. Quantification of termite bioturbation in a savannah ecosystem: Application of OSL dating. Quaternary Geochronology 30, 334-341.
Kumar, M., 2009. Excavations at Madina district, Rohtak, Haryana 2007-08: a report. In: Osada, T., Uesugi, A. (eds.) Linguistics Archaeology and the Human Past. Research Institute for Humanity and Nature, 1–75.
Kunz, A., Frechen, M., Ramesh, R., Urban, B., 2010. Luminescence dating of late Holcene dunes showing remnants of early settlement in Cuddalore and evidence of monsoon activity in south east India. Quaternary International 222, 194-208.
Lyons, R., Tooth, S., Duller, G.A.T., 2014. Late Quaternary climatic changes revealed by luminescence dating, mineral magnetism and diffuse reflectance spectroscopy of river terrace palaeosols: a new form of geoproxy data for the southern African interior. Quaternary Science Reviews 95, 43-59.
MacDonald, G., 2011. Potential influence of the Pacific Ocean on the Indian summer monsoon and Harappan decline. Quaternary International 229, 140-148.
Madella, M., Fuller, D.Q., 2006. Palaeoecology and the Harappan Civilisation of South Asia: a reconsideration. Quaternary Science Reviews, 25, 1283-1301.
Maemoku, H., Shitaoka, Y., Natomo, T., Yagi, H. 2012. Geomorphological Constraints on the Ghaggar River Regime During the Mature Harappan Period. In Giosan, L., Fuller, D.Q., Nicoll, K., Flad, R.K., Clift, P.D. (eds.), Climates, landscapes, and civilizations: American Geophysical Union Geophysical Monograph 198, pp. 97-106.
Morrill, C., Overpeck, J.T., Cole, J.E., 2003. A synthesis of abrupt changes in the Asian summer monsoon since the last deglaciation. The Holocene 13, 465-476.
Mehdi, S.M., Pant, N.C., Saini, H.S., Mujtaba, S.A.I., Pande, P., 2016. Identification of palaeochannel configuration in the Saraswati River basin in parts of Haryana and Rajasthan, India, through digital remote sensing and GIS. Episodes, 39, 29-38.
Mughal, M. R., 1997. Ancient Cholistan: archaeology and architecture. Ferozsons, Lahore.
Murray, A.S., Wintle, A.G., 2000. Luminescence dating of quartz using an improved single-aliquot regenerative-dose protocol. Radiation Measurements 32, 57-73.
Nathan, R.P., Thomas, P.J., Jain, M., Murray, A.S., Rhodes, E.J., 2003. Environmental dose rate heterogeneity of beta radiation and its implications for luminescence dating: Monte Carlo modelling and experimental validation. Radiation Measurements 37, 305–313.
Olley, J.M., Pietsch, T., Roberts, R.G., 2004. Optical dating of Holocene sediments from a variety of geomorphic setting using single grains of quartz, Geomorphology 60, 337–358
Orengo, H.A. and Petrie, C.A., 2017. Large-Scale, Multi-Temporal Remote Sensing of Palaeo-River Networks: A Case Study from Northwest India and its Implications for the Indus Civilisation. Remote Sensing, 9, 735.
Parton, A., Farrant, A.R., Leng, M.J., Telfer, M.W., Groucutt, H.S., Petraglia, M.D., 2015. Alluvial fan records from southeast Arabia reveal multiple windows for human dispersal. Geology, 43, 295-298.
Petrie C.A., 2013. South Asia. In Clark, P. (ed.) The Oxford Handbook of Cities in World History. Oxford, Oxford University Press, pp. 83-104.
Petrie, C.A., 2017. Crisis, what crisis? Adaptation, resilience and transformation in the Indus Civilisation. In: Dreisen, J., Cunningham, T. (eds.) Crisis to collapse: the Archaeology of social breakdown. Aegis Publications, UC Louvain.
Petrie, C.A., Bates, J., 2017. ‘Multi-cropping’, intercropping and adaptation to variable environemnts in Indus South Asia. Journal of World Prehistory, 30, 81-130.
Petrie, C.A., Khan, F., Knox, J.R., Thomas, K.D. & Morris, J.C. 2010. The investigation of early villages in the hills and on the plains of western South Asia, in Petrie, C.A. (ed.). Sheri Khan Tarakai and early village life in the borderlands of north-west Pakistan, Bannu Archaeological Project Monographs - Volume 1, Oxbow Books, Oxford: 7-28.
Petrie, C.A., Singh, R.N., Bates, J., Dixit, Y., French, C.A.I, Hodell, D., Jones, P.J., Lancelotti, C., Lynam, F., Neogi, S., Pandey, A.K., Parikh, D., Pawar, V., Redhouse, D.I., Singh, D.P., 2017. Adaptation to variable environments, resilience to climate change: investigating Land, Water and Settlement in northwest India. Current Anthropology, 58, 1-30.
Possehl, G.L., 2002. The Indus civilisation: a contemporary perspective. Altamira Press, California.
Prasad, S., Enzel, Y., 2006. Holocene paleoclimates of India. Quaternary Research 66, 442-453.

569 Prasad, S., Kusumgar, S., Gupta, S.K., 1997. A mid-late Holocene record of palaeoclimatic changes from Nal
570 Sarovar – A palaeodesert margin lake in western India. Journal of Quaternary Science 12, 153-159.
571 Radhakrishna, B.P., Merh S.S., 1999. Vedic Saraswati: evolutionary history of a lost river of Northwestern
572 India. Geological Society of India, Delhi.
573 Rowan, A.V., Roberts, H.M., Jones, M.A., Duller, G.A.T., Covey-Crump, S.J., Brocklehurst, S.H., 2012.
574 Optically stimulated luminescence dating of glaciofluvial sediments on the Canterbury Plains, South
575 Island, New Zealand. Quaternary Geochronology 8, 10-22.
576 Sahai, B., 1999. Unravelling the lost Saraswati. In: Radhakrishna, B.P., Merh, S.S. (eds.). Vedic Saraswati:
577 evolutionary history of a lost river of Northwestern India. Geological Society of India, 42, 121-141.
578 Saini, H.S., Mujtaba, S.A.I., 2010. Luminescence dating of the sediments from a buried channel loop in
579 Fatehabad area, Haryana: insight into vedic Saraswati River and its environment. Geochronometria 37,
580 29-35.
581 Saini, H.S., Tandon, S.K., Mujtaba, S.A.I., Pant, N.C., Khorana, R.K., 2009. Reconstruction of buried channel-
582 floodplain systems of the northwestern Haryana Plains and their relation to the 'Vedic' Saraswati.
583 Current Science 97, 1634-1643.
584 Shitaoka, Y., Maemoku, H., Nagatomo, T., 2012. Quartz OSL dating of sand dunes in Ghaggar Basin,
585 northwestern India. Geochronometria 39, 221-226.
586 Singh, R.N. and Petrie, C.A. 2009. Lost rivers and life on the plains – approaches to understanding
587 human/environment interaction between the collapse of Indus urbanism and the rise of the Early
588 Historic cities (The Land, Water and Settlement Project), Sarasvati River - A Perspective. Conference
589 Proceedings, Kurukshetra University, Kurukshetra, 102-111.
590 Singh, R.N., Petrie, C.A., Pawar, V., Pandey, A.K., Neogi, S., Singh, M., Singh, A.K. Parikh, D. and Lancelotti, C.
591 2010. Changing patterns of settlement in the rise and fall of Harappan urbanism: preliminary report on
592 the Rakhigarhi Hinterland Survey 2009, Man and Environment 35.1, 37-53.
593 Singh, R.N., Petrie, C.A., Pawar, V., Pandey, A.K. and Parikh, D. 2011. New insights into settlement along the
594 Ghaggar and its hinterland: a preliminary report on the Ghaggar Hinterland Survey 2010, Man and
595 Environment 36.2, 89-106.
596 Singh, R.N., Petrie, C.A., French, C.A., Bates, J., Pandey, A.K., Parikh, D., Lancelotti, C. and Redhouse, D.I.
597 2012. Survey and excavations at Dabli-vas Chugta, Hanumangarh District, Rajasthan. Puratattva 42, 133-
598 147.
599 Singh, A., Paul, D., Sinha, R., Thomsen, K.J., Gupta, S., 2016. Geochemistry of buried river sediments from
600 Ghaggar Plains, NW India: Multi-proxy records of variations in provenance, paleoclimate, and
601 paleovegetation patterns in the Late Quaternary. Palaeogeography, palaeoclimatology, palaeoecology
602 449, 85-100.
603 Singh, G., 1971. The Indus Valley culture seen in the context of postglacial climatic and ecological studies in
604 north-west India. Archaeology and Physical Anthropology of Oceania, 6, 177-189.
605 Singh, G., Joshi, R.D., Singh, A.B., 1972. Stratigraphic evidence for the age and development of three salt
606 lake deposits in Rajasthan, India. Quaternary Research 2, 496-505.
607 Singh, G., Joshi, R.D., Singh, A.B., 1973. Pollen-rain from the vegetation of northwest India. New Phytologist
608 72, 191-206.
609 Singh, G., Joshi, R.D., Chopra, S.K., Singh, A.B., 1974. Late Quaternary history of vegetation and climate in
610 the Rajasthan Desert, India. Philosophical Transactions of the Royal Society of London 267, 467-501.
611 Singh, G., Wasson, R.J., Agrawal, D.P., 1990. Vegetational and seasonal climatic changes since the last full
612 glacial in the Thar Desert, Northwestern India. Review of Palaeobotany and Palynology, The Proceedings
613 of the 7th International Palynological Congress , 64, 351-358.
614 Singhvi, A.K. and Kar, A., 2004. The aeolian sedimentation record of the Thar Desert. Proceedings of the
615 Indian Academy of Science, 113, 371-401.
616 Singhvi, A.K., Williams, M.A.J., Rajaguru, S.N., Misra, V.N., Chawla, S., Stokes, S., Chauhan, N., Francis, T.,
617 Ganjoo, R.K., Humphreys, G.S., 2010b. A ~200 ka record of climatic change and dune activity in the Thar
618 Desert, India. Quaternary Science Reviews 29, 3095-3105.
619 Sinha, R., Yadav, G.S., Gupta, S., Singh, A., Lahiri, S.K., 2013. Geo-electric resistivity evidence for subsurface
620 palaeochannel systems adjacent to Harappan sites in northwest India. Quaternary International 208, 66-
621 75.
622 Sood, R.K., Sahai, B., 1983. Hydrographic changes in northwestern India. Man and Environment 7, 166-169.

623 Srivastava, P., Juyal, N., Singhvi, A.K., Wasson, R.J., Bateman, M.D., 2001. Luminescence chronology of river
624 adjustment and incision of Quaternary sediments in the alluvial plain of the Sabarmati River, north
625 Gujarat, India. Geomorphology 36, 217-229.
626 Staubwasser, M., Weiss, H., 2006. Holocene climate and cultural evolution in late prehistoric-early historic
627 West Asia. Quaternary Research 66, 372-387.
628 Staubwasser, M., Sirocko, F., Grootes, P.M., Segl. M., 2003. Climate change at the 4.2 ka BP termination of
629 the Indus valley civilisation and Holocene south Asian monsoon variability. Geophysical Research Letters
630 30, doi:10.1029/2002GL016822.
631 Stein, M.A., 1942. A survey of ancient sites along the 'lost' Sarasvati River. Geographical Journal 99, 173-
632 182.
633 Tandon, S.K., Sareen, B.K., Someshwar Rao, M., Singhvi, A.K., 1997. Aggradation history and luminescence
634 chronology of Late Quaternary semi-arid sequences of the Sabarmati basin, Gujarat, Western India.
635 Palaeogeography, palaeoclimatology, palaeoecology 128, 339-357.
636 Thomas, D.S.G., 2013. Reconstructing palaeoenvironments and palaeoclimates in drylands: what can
637 landform analysis contribute? Earth Surface Processes and Landforms, 38, 3-16.
638 Thomas, D.S.G. and Burrough, S.L., 2016. Luminescence-based dune chronologies in southern Africa:
639 Analysis and interpretation of dune database records across the subcontinent. Quaternary International,
640 410, 30-45.
641 Thomas, J.V., Kar, A., Kailath, A. J., Juyal, N., Rajaguru, S.N. and Singhvi, A.K., 1999. Late Pleistocene -
642 Holocene history of aeolian accumulation in the Thar desert, India. Zeitschrift fur Geomorphologie
643 Supplement Band, 116, 181–194.
644 Thomas, P.J., Juyal, N., Kale, V.S., Singhvi, A.S., 2007. Luminescence chronology of late Holocene extreme
645 hydrological events in the upper Penner River basin, South India. Journal of Quaternary Science 22, 747-
646 753.
647 Wang, Y., Cheng, H., Edwards, R.L., He, Y., Kong, X., An, Z., Wu, J., Kelly, M.J., Dykoski, C.A., Li, X., 2005. The
648 Holocene Asian Monsoon: links to solar changes and North Atlantic climate. Science 308, 854-857.
649 Wasson, R.J., 1984. The sedimentological basis of the Mohenjo-Daro flood hypothesis. Man and
650 environment 8, 88-90.
651 Weber, S.A., Barela, T., Lehman, H., 2010. Ecological continuity: an explanation for agricultural diversity in
652 the Indus Civlisation and beyond. Man and Environment, 35, 62-25.
653 Wilhelmy, H., 1969. The ancient river valley on the eastern border of the Indus Plain and the Saraswati
654 problem. Zeitschrift fur Geomorphologie 8, 76-93.
655 Wintle, A.G., Murray, A.S., 2006. A review of quartz optically stimulated luminescence characteristics and
656 their relevance in single-aliquot regeneration dating protocols. Radiation Measurements 41, 369-391.
657 Wright, R.P., 2010. The ancient Indus. Cambridge University Press, Cambridge.
658 Wright, R.P., Bryson, R.A., Schuldenrein, J., 2008. Water supply and history: Harappa and the Beas regional
659 survey. Antiquity 82, 37-48.
660 Yash Pal, Sahai, B., Sood, R.K., Agrawal, D.P., 1980. Remote sensing of the 'Lost' Saraswati River.
661 Proceedings of the Indian Academy of Science 89, 313-331.

Figure Captions

Figure 1: Study and sample location, position of major regional fluvial systems and Indus Civilisation sites (white, closed symbols). Major Indus urban centres are highlighted, the sites sampled in this study are indicated by the triangle symbols. The area shown in figure 2 is also highlighted.

Figure 2: Satellite image of the study area and sampled sites. OSL ages (ka) are shown, as well as a schematic view of the site stratigraphic logs. Sample depths are in metres. Local settlements mentioned in the main text are shown.

Figure 3: Examples of a) an aeolian site (IND-14-1) and b) a fluvial site (IND-14-9). At site IND-14-1, fine silty sands were found which fine slightly towards the base of the unit. Some small, sporadic calcrete nodules were observed, but avoided for OSL sampling. At site IND-14-9, silty sands have accumulated in a homogenous unit with some very fine laminations observable in the upper part of the sequence.

Figure 4: Sediment grain size distribution data by volume for selected aeolian samples (a) and fluvial samples (b). The median grain size for each sample is shown by the opaque symbol.

Figure 5: a) Typical OSL signal and dose response curve (inset) from a single grain of quartz from sample IND-14-1-1 with an equivalent dose of approximately 12 Gy. b) Radial plot of D_e distribution of IND-14-1-1. The sample D_e of 5.37 Gy is shown by the solid line and ±2σ by the grey shaded area.

Figure 6: a) Summer insolation (W/m2) at 30°N (from Berger and Loutre, 1999). b) 18O record (‰ VPDB (Vienna Peedee belemnite)) from Mawmulah Cave, northeast India (from Berkelhammer et al., 2012). c) Foraminiferal 18O record (‰ VPDB) from the Indus Delta (Staubwasser et al., 2003). d) Gastropod 18O record (‰ VPDB) from Kotla Dahar lake (black; Dixit et al., 2014a) and Riwasa lake (grey; Dixit et al., 2014b). e) The OSL ages and uncertainties calculated in this study. Black symbols are from aeolian sediments and grey symbols from fluvial.

685 **Figure 1**

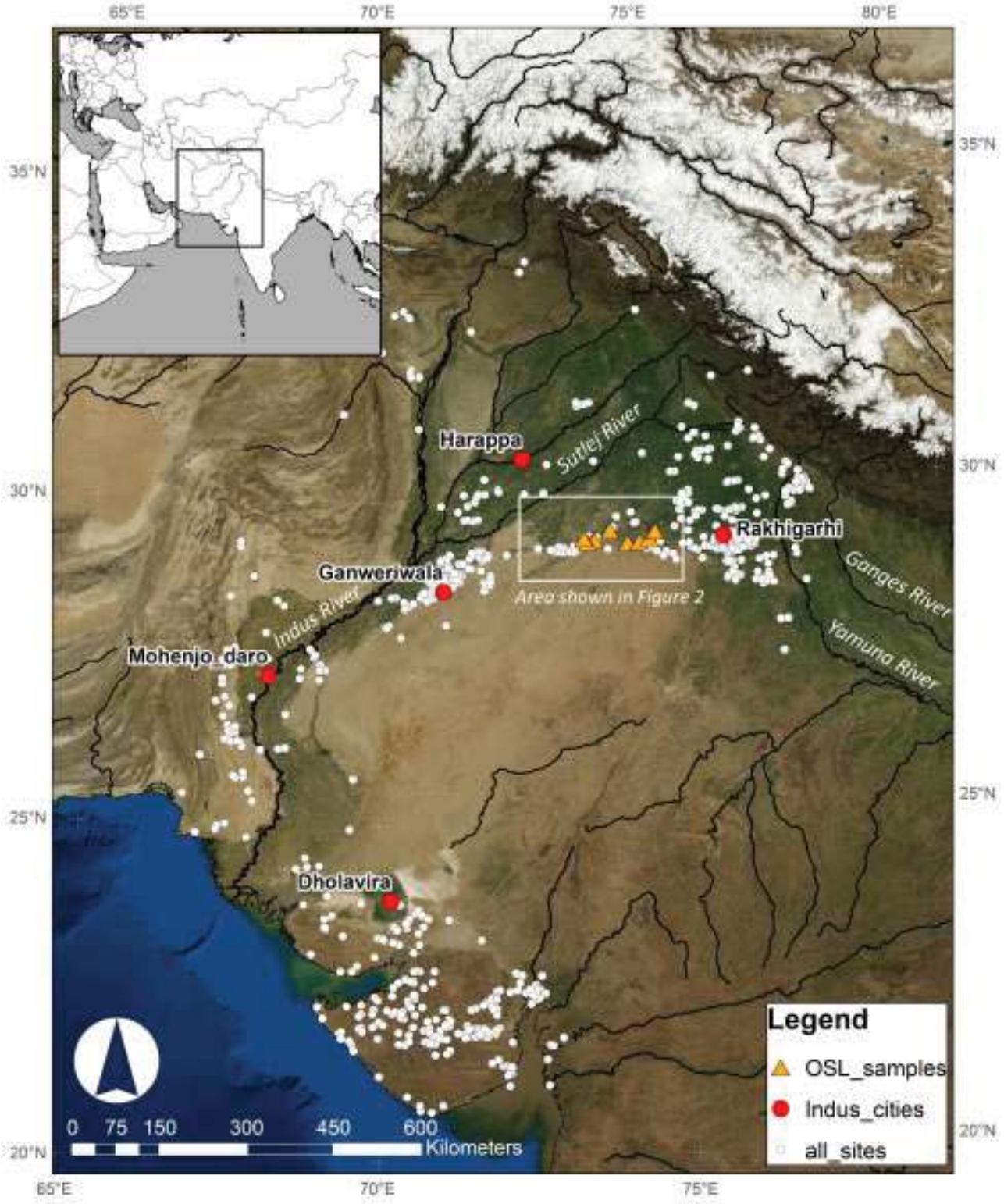

686
687

688 **Figure 2**

689

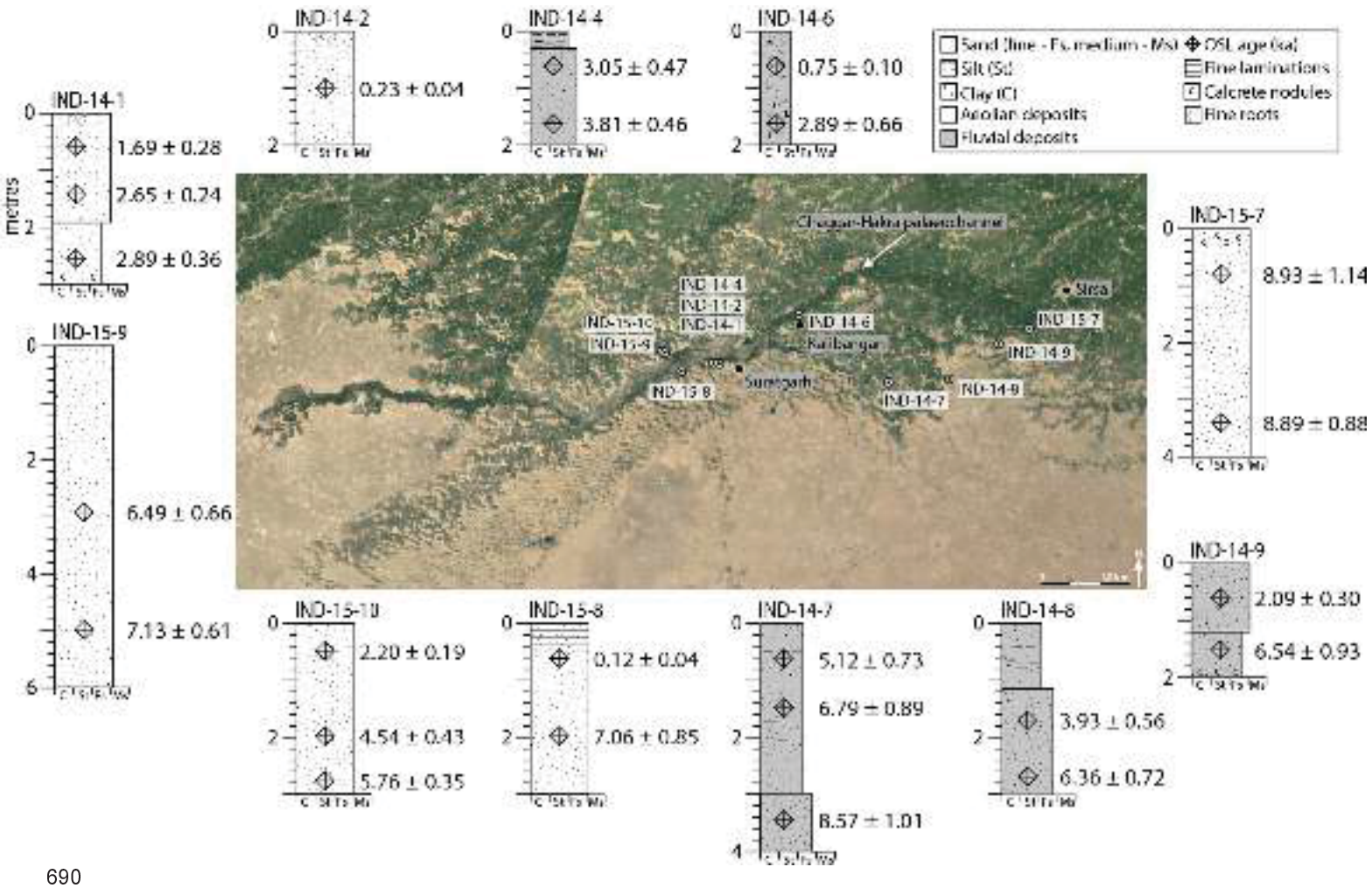

690

691

692 **Figure 3**

693

694

695

696 **Figure 4**

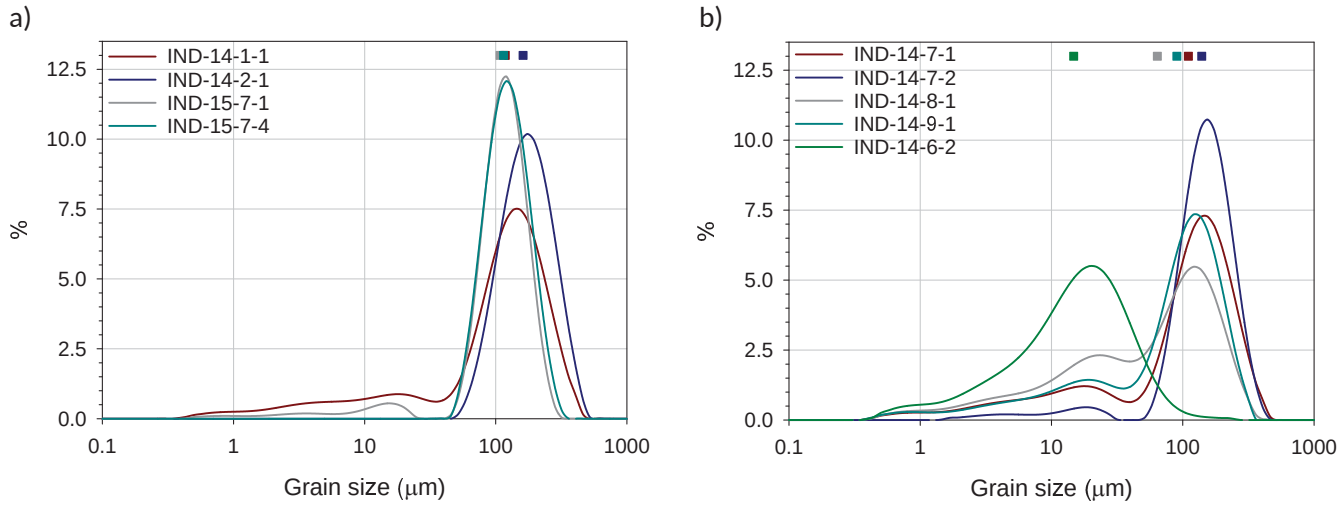

697

698

699 **Figure 5**

700

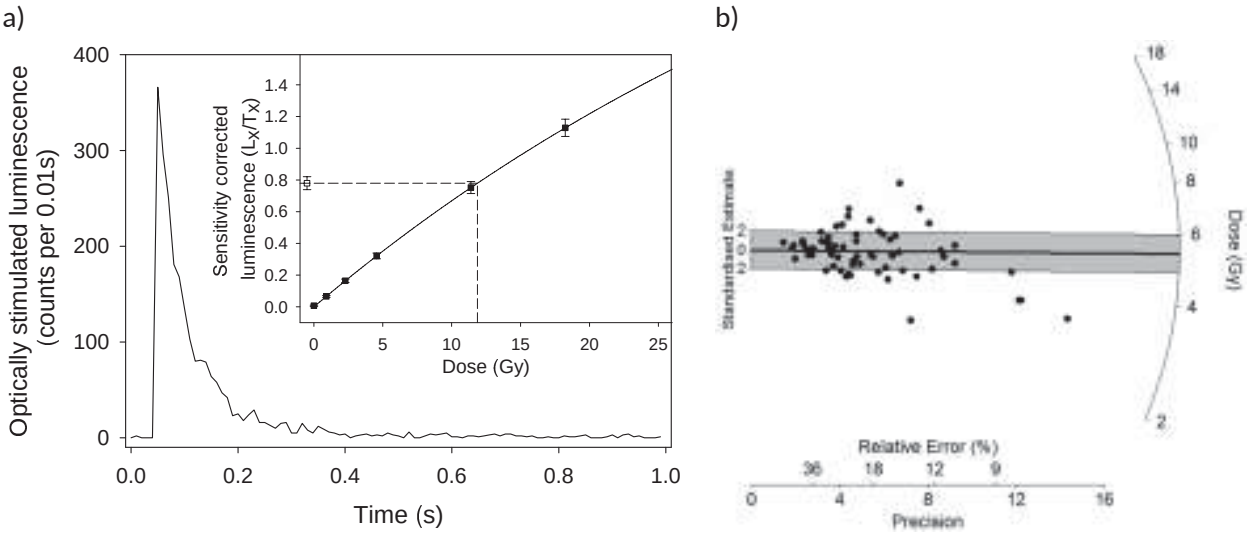

701

702

703 **Figure 6**

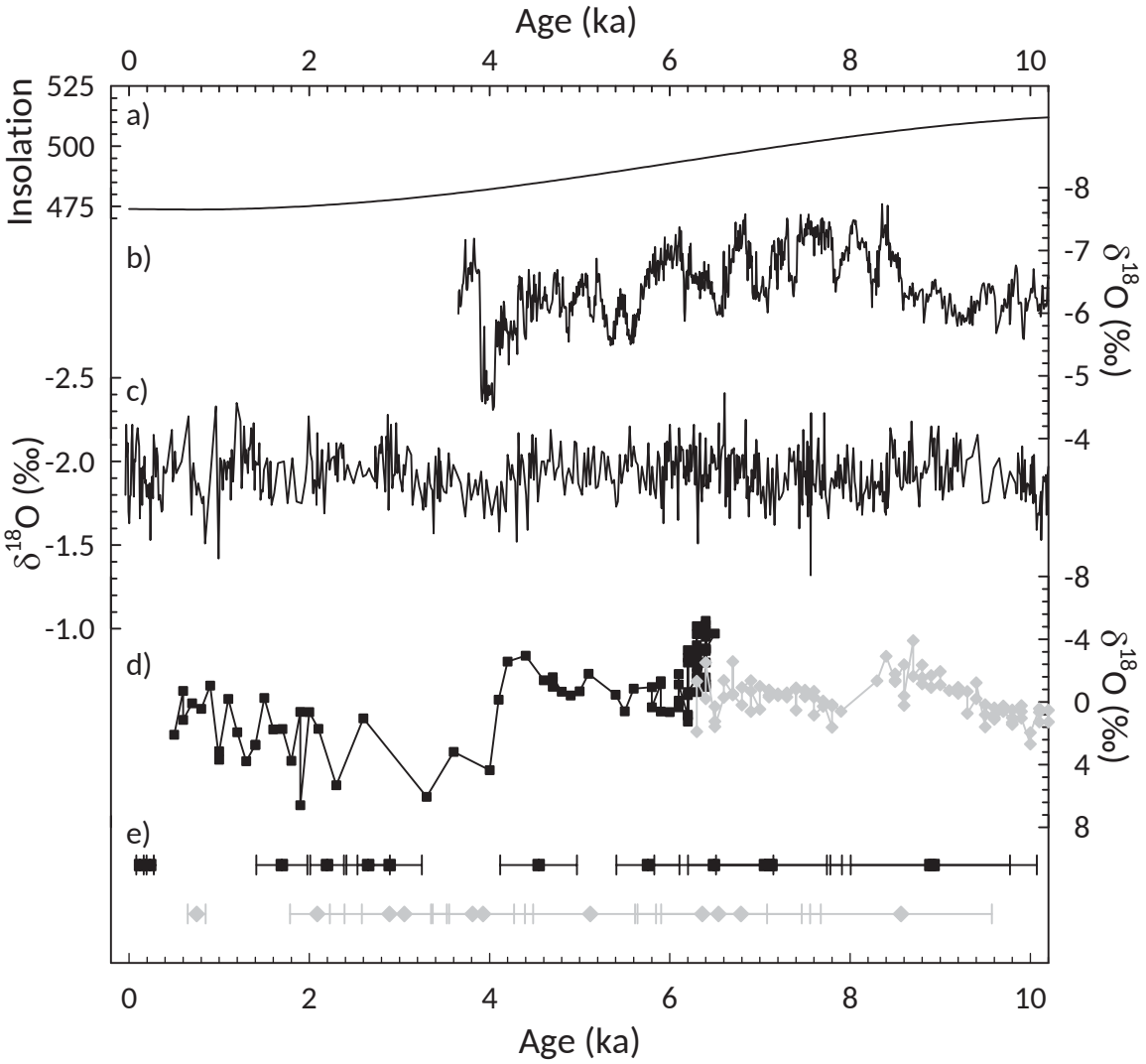

704
705

AUTHOR DECLARATION TEMPLATE

We wish to confirm that there are no known conflicts of interest associated with this publication and there has been no significant financial support for this work that could have influenced its outcome.

We confirm that the manuscript has been read and approved by all named authors and that there are no other persons who satisfied the criteria for authorship but are not listed. We further confirm that the order of authors listed in the manuscript has been approved by all of us.

We confirm that we have given due consideration to the protection of intellectual property associated with this work and that there are no impediments to publication, including the timing of publication, with respect to intellectual property. In so doing we confirm that we have followed the regulations of our institutions concerning intellectual property.

We understand that the Corresponding Author is the sole contact for the Editorial process (including Editorial Manager and direct communications with the office). He/she is responsible for communicating with the other authors about progress, submissions of revisions and final approval of proofs. We confirm that we have provided a current, correct email address which is accessible by the Corresponding Author and which has been configured to accept email from julie.durcan@ouce.ox.ac.uk

Signed by all authors as follows:

Julie Durcan on 15/12/2016

on behalf of co-authors:

Professor David Thomas

Professor Sanjeev Gupta

Dr Vikas Pawar

Dr Ravindra Singh

Dr Cameron Petrie